Journal of the Korean Society of Marine Environment & Safety
Research Paper
Vol. 23, No. 1, pp. 104-111, February 28, 2017, ISSN 1229-3431(Print) / ISSN 2287-3341(Online) https://doi.org/10.7837/kosomes.2017.23.1.104

Internal Flow Analysis of Seawater Cooling Pump using CFD

Ngoc Tran Bao* · Chang-jo Yang** · Bu-gi Kim*** · Jun-ho Kim***†
* Graduate School of Mokpo National Maritime University, Mokpo 58628, Korea
** Division of Marine Engineering, Mokpo National Maritime University, Mokpo 58628, Korea
*** Division of Mechatronics Engineering, Mokpo National Maritime University, Mokpo 58628, Korea

CFD를 이용한 해수냉각펌프의 내부유동 분석

Ngoc Tran Bao* · 양창조** · 김부기*** · 김준호***†
* 목포해양대학교 대학원, ** 목포해양대학교 기관시스템공학부, *** 목포해양대학교 해양메카트로닉스학부

Abstract : *This research focuses on simulation and visualization of flow field characteristics inside a centrifugal pump. The 3D numerical analysis was carried out by using a numerical CFD tool, addressing a Reynolds Average Navier-Stock code with a standard k-ε two-equation turbulence model. The simulation accounts for friction head loss due to rough walls at suction, impeller, discharge areas and volumetric head loss at impeller wear ring. A comparison of performance curves between simulation and experimentation is included, and it reveals a same trend of those results with a small difference of maximum 5%. At best efficiency point, velocity vectors are smooth but it changes significantly under off-design point, a strong recirculation appears at the outlet of impeller passages near tongue area. A relatively uniform preassure distribution was observed around the impeller in despite of the tongue. Within the volute, because of its geometry, spiral vortexes formed, proving that the flow field in this region was relatively turbulent and unsteady.*

Key Words : *Centrifugal pump, CFD, Velocity field, Pressure distribution, Vortex formation*

요 약 : 본 연구는 원심펌프 내부 유동장 특성에 대한 시뮬레이션 및 시각화에 중점을 둔다. 3D 수치해석은 Reynolds Average Navier-stock 코드를 k-ε 표준 2차방정식 난류 모델로 처리하여 수행하였다. 시뮬레이션은 흡입측, 임펠러, 토출측 영역에서 조도로 인한 마찰 손실과 임펠러 웨어링에서 체적 손실을 포함한다. 해석과 실험사이의 성능곡선 비교결과 최대 5%의 작은 차이를 보이며 동일한 추세를 나타냈다. 최고 효율점에서 속도 벡터는 고르게 나타났지만 비 설계점에서는 현저한 변화가 나타났고, 텅 부근의 임펠러 유로 토출부에서 강력한 재순환 영역이 나타났다. 비교적 일정한 압력분포가 텅 부근임에도 불구하고 임펠러 주위에 관찰되었다. 볼류트 내에서 기하학적으로 인해 형성된 나선형 와류가 이 영역에서 유동장이 상대적으로 난류이고 불안정하다는 것을 증명하였다.

핵심용어 : 원심펌프, 전산유체역학, 속도장, 압력분포, 와류형성

1. Introduction

Being as the most common type of pump used for several applications in industries, agriculture and other sectors, centrifugal pumps attract numerous concerns from not only manufacturers, engineers but also employers. Centrifugal pump is a type of turbo machinery converting mechanical energy into pressure energy by means of centrifugal force acting on the fluid. It possesses the capability to operate with higher flow rate and higher efficiency compared to other types of pump such as axial pump and displacement reciprocating pump. The pump which is investigated in this research is a sea water cooling pump used on board a ship namely MS125A. The main propulsion and other auxiliary machineries generate heat due to combustion and other processes involved in performing of their operations. This heat has to be transferred to some medium, so that the machineries can function properly within safe operating parameters. Main and auxiliary machineries are cooled with sea water conveyed from sea chest by sea water cooling pump. This pump is in charged of circulating

* First Author : ngoctranbao.hn@gmail.com, 061-240-7472
† Corresponding Author : junho.kim@mmu.ac.kr, 061-240-7241

sea water throughout the pant and throwing out water after it extracts the heat from machineries.

In the design process, before putting a pump into actual use, the performance of internal flow in the entire pump needs to be predicted in order to ensure high demand operations. This requires critical analysis of highly complex and turbulent flow inside the pump. Simulation done by CFD gives us a great opportunity to visualize flow condition inside centrifugal pumps as well as provides precious information to facilitate design work. Based on simulation results, engineers easily predict pump's characteristics which lead to a reduction in time and progress to take place experiments. Nevertheless, the complicated flow filed such as vortex formation, geometry-based separation, and impeller-volute interaction is difficult to control and obtain due to the rotating and stationary components. Byskov (Byskov et al., 2003) carried out an analysis on a six-bladed impeller by using the large eddy simulation (LES) at design and off-design conditions. At design point, the flow field inside the impeller is smooth with no significant separation. At quarter design load, a steady non-rotating stall phenomenon is observed in the entrance and a relative eddy is developed in the remaining area of the passage. Bacharoudis (Bacharoudis et al., 2008) investigated the flow mechanisms inside centrifugal impeller and studied performance by varying outlet blade angle. When increasing the outlet blade angle from 20^{o} to 45^{o}, an improvement in head more than 7 % is observed. Gu (Gu et al., 2001) has contributed to reveal the volute-diffuser interaction of a single stage centrifugal compressor and found that at higher flow rate than design point, a twin vortex structure is formed downstream of the passage. With the aid of advancing computer, significant improvement of numerical algorithms and more reliable CFD codes, a great deal of labour and facility will be saved. We can believe in an increasing trend of applying numerical methods to study the complex flow in centrifugal pumps so as to improve efficiency and shorten the design process.

Several researchers have analyzed a centrifugal pump by solving Navier-Stock equations, coupled with the standard k-e turbulence model. However, they did not take the effect of leakage flow at impeller wear ring into account, and they considered the roughness of domain wall as smooth wall. Therefore, this current research focuses on investigating the centrifugal pump performance, velocity field and pressure distribution inside the pump in both design and off-design operations, accounting for friction head loss (on the domain wall) and volumetric head loss (at wear ring clearance).

2. Pump specification

2.1 Pump specification

The first task on a numerical flow simulation is to define the geometry, followed by to generate grid. This is one of the most important steps in simulation work. The whole pump under investigation is shown in Figure 1, including a close type impeller, a leakage flow (at impeller clearance), a curved intake section with swirl breaker, and a spiral volute casing. The impeller consists of seven curvature backward swept blades of constant thickness with arc profile leading edge and blunt trailing edge. Axial high of the impeller blade is tapered from 46.93 mm at the inlet to 20.51 mm at the outlet. The impeller outer diameter d_2 is 284 mm, with an outlet width b_2 of 20 mm. The flow from impeller is discharged in to a spiral volute casing with mean circle diameter d_3 of 297 mm.

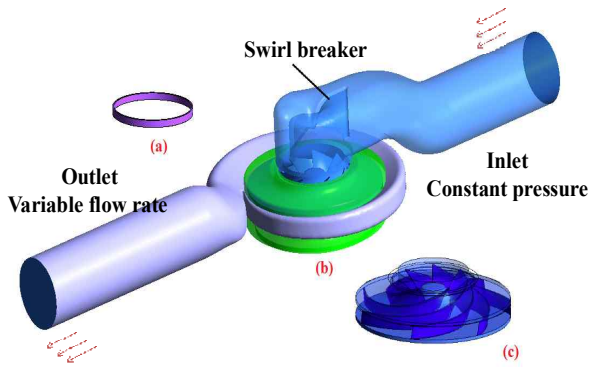

(a) leakage flow, (b) pump assembly, (c) impeller

Fig. 1. MS125A Pump geometry.

Table 1. Pump Design parameters

Parameter	Sign	Value	Unit
Inlet diameter of impeller	d_1	60	mm
Outlet diameter of impeller	d_2	284	mm
Number of blades	Z	7	-
Outlet blade angle	β_2	28	^{o}
Outlet width of impeller	b_2	20	mm
Blade passing frequency	f_{BP}	204	Hz
Clearance at impeller wear ring	cl	0.25	mm
Diameter of cut-water	d_3	297	mm
Volute width	b_3	34	mm
Outlet flange diameter	ϕ_{Outlet}	125	mm

The impeller is designed to rotate at 1780 rpm with a specific speed of 140. At best efficiency point (BEP), the designed flow rate is 140 m^3/h, and the designed head is 41m. The side chamber clearance between impeller and casing is also included to take the effect of leakage flow in to account. The main pump parameters are described in Table 1.

2.2 Grid sensitivity

The mesh of unstructured tetrahedra grid was created for the whole geometry (except leakage flow domain which is based on hexahedron grid) using ICEM-CFD 15.1. The pump includes four main parts: suction domain, impeller domain, volute domain and leakage flow domain. Each of them was built and meshed independently.

To validate the accuracy of numerical computation, it was essential to carry out a mesh sensitivity study of computational domains. In terms of theoretical aspect, the finer the mesh is, the fewer grid-related errors are (Ferziger and Peric, 1996). Here, the head coefficient at design flow condition was taken as standard parameter to evaluate five grids and determined the impact of mesh size on the solution accuracy. The same turbulence model (k-e) was used to compare head coefficient of each case.

Table 2. Detail of grid size

Domain	Case 1	Case 2	Case 3	Case 4	Case 5
Suction	386,952	489,331	802,641	1,065,504	1,264,512
Impeller	953,684	1,243,295	1,923,655	2,536,933	2,946,353
Leakage Flow	86,321	132,658	163,059	214,560	312,652
Volute	416,351	690,366	870,144	1,146,311	1,304,539
Total	1,843,308	2,555,650	3,759,499	4,963,338	5,827,058

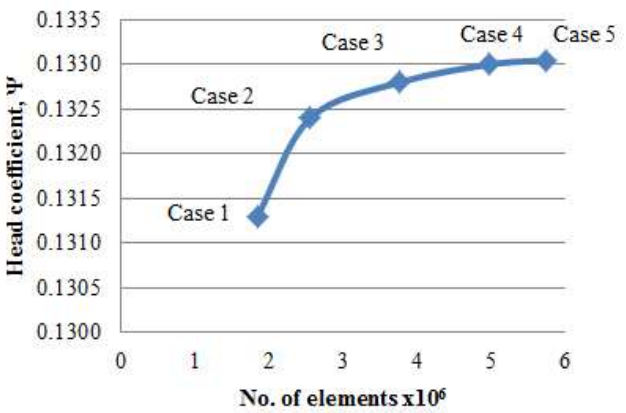

Fig. 2. Impact of grid size on head coefficient.

The grid independence study was taken place in five cases according to five mesh sizes from case 1 to case 5. Detail of elements' number of each grid and the influent of grid size on head coefficient were demonstrated on Table 2 and Figure 2, respectively. It can be clearly seen from Figure 2 that the pump head coefficient increases when applying finer mesh, reaching an asymptotic value at the quantity of elements of 4,960,000. In terms of case 5, the head coefficient slightly increases in spite of a large change in number of elements. Base on this figure, grid size of case 4 with total 4,960,000 elements is considered to be reliable to ensure the grid independent and simulation accuracy.

3. Numerical method

3.1 Turbulence model

In this computational analysis, a commercially available CFD code-CFX is employed to investigate the complex three-dimensional turbulence flow through the centrifugal pump. CFX, which was utilized by a handful of researchers, is a multi-purpose CFD code to solve three dimensional Reynolds Average Navier-Stock (RANS) equation for steady and turbulent fluid flow. Validation of this code can be seen in studies done by Majidi and Siekmann (Majidi and Siekmann, 2000), Gu (Gu et al., 2001), and Asuaje (Asuaje et al., 2006) who have applied it on turbo machinery numerical computation. According to turbulence model studies conducted by K. W. Cheah (Cheah et al., 2011), there is no significant discrepancy in head coefficient observed from different simulations with 3 widely used turbulence models: k－e, k-ω, SST (Shear Stress Transport). Therefore, standard k－e turbulence model with log-law wall function is chosen for present research due to fast convergence time. The current numerical computation is carried out with a multiple frames of reference approach as the suction, volute, and leakage flow domain are in stationary frame meanwhile impeller domain is in rotating frame. The grid of four computational domains including suction, leakage flow, impeller, and volute are created separately. The unstructured mesh with tetrahedra elements is used by dint of the complexity and irregular profile of suction, impeller and volute domain. Whereas, leakage flow domain employs structured mesh based on hexa-hedra elements. A local refinement of mesh is applied at some important regions such as: volute tongue area, leading and trailing edges of

impeller blades so as to precisely capture flow field structure. It is believed that flow field properties including velocity and pressure at those areas are expected to be substantial. The number of elements of each domain is fixed after conducting mesh independent study.

3.2 Boundary condition

The original configuration of casing is slightly modified in order to avoid the existence of large recirculation in some areas. The extensions of 2D at suction domain and 3D at volute-discharge domain are essential for numerical and physical reasons, because convergence problems and related flow instabilities can be prevented. In this numerical simulation, multiple frames of reference were involved. Impeller domain is set in rotational frame of reference, while three remaining domains belong to stationary frame. The interfaces between rotational and stationary components are set as frozen-rotor type, and ones between two stationary domains are set as general connection. Two frames of reference, rotating and stationary, are connected in such a way that for steady state analysis the relative position of impeller and volute domain does not change by the time.

Boundary conditions specify the flow and thermal variables on the boundary of physical model. Present study is based on steady state analysis with the following boundary conditions imposed: at the inlet of suction domain a constant total pressure is set, and turbulent intensity is specified to be 5 %. As for outlet BC, variable mass flow rates ranging from $0.4Q_{design}$ to $1.4Q_{design}$ are applied (shown on Fig. 1). Rough wall condition is imposed on all the wall of every domain with a value of 0.01 mm. Water in ambient condition is used as a working fluid.

4. Results and discussion

4.1 Pump performance curves

Figure 3 shows head – flow coefficient curve and efficiency – flow coefficient curve of surveyed pump, respectively. It can be observed from the chart that globally the head coefficient and efficiency of simulation results follow the same trend as experiment results. Two numerically predicted performance curves getting from steady simulation over a wide range of flow rate are in quite good agreement with experiment curves, that similar to results offered by Cheah (Cheah et al., 2011).

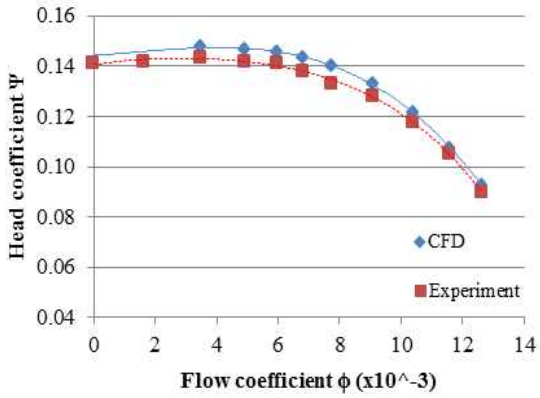

(a) Head coefficient curve

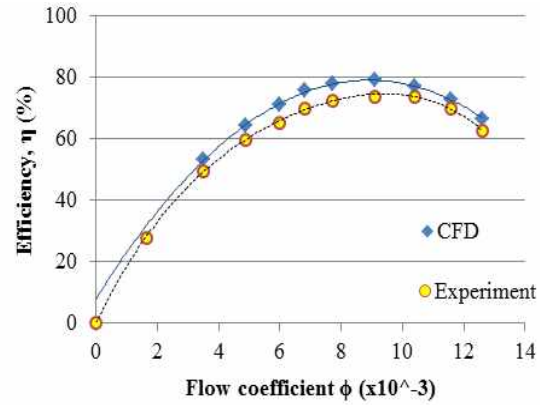

(b) Efficiency curve

Fig. 3. Performance curves of model pump.

In terms of head-flow coefficient chart, the numerical estimated Ψ at Q_{design} is 0.1330 compared to experiment Ψ of 0.1278, accounting for a discrepancy of 4.1 %. This difference is due to other types of head loss in actual operating condition. In this study friction head loss and volumetric head loss are taken into consideration, nonetheless there are some other kinds of head loss which cannot be calculated accurately in detail. If those kinds of head loss are included in centrifugal pump modeling, a better agreement between simulation and experiment will be able to achieve. Meanwhile, efficiency curve witnesses a disparity of 5 % between experimental and numerical result. The actual best efficiency of the pump is 74 % but the simulation predicted efficiency is at 79 %. It seems reasonable because in reality the impeller consumes more power than in calculation which results in a higher predicted efficiency.

In computational simulation, the flow rate cannot be reduced under the critical value $\phi = 0.00351$ because of the convergence problem caused by large recirculation within volute casing and

impeller passages. At lower flow rate, the numerical computation over predicts loss brought by high turbulence and large recirculation, and as a result the discrepancy between actuality and simulation will go up.

4.2 Velocity field

Figure 4 shows the geometry of suction domain and the position of 6 planes where we investigate the velocity flow field. Figure 5 illustrates the variation of velocity vector on some planes to visualize the way the pre-swirl flow developed upstream before entering impeller eye. Location of each plane can be clearly seen on the picture, the declinations of plane 3 to 6 (compared to vertical direction) are 30^o, 40^o, 50^o and 80^o, respectively.

Starting from the beginning of suction domain, the flow on two first planes is very smooth and uniform. When approaching the rectangular shape region, there is an existence of low velocity particles on plane 3 and 4 which is a signal of flow separation. Nevertheless, with the aid of swirl breaker the pre-swirl flow is blocked and only appears at the top of plane. Further downstream on plane 5, the vortex flow structure develops stronger and vortex formation is distinct near top wall region. Because of the sudden change in flow direction, the formation of swirl flow is unavoidable. The swirl breaker in suction domain plays an essential role in reducing the adverse impacts of vortex on flow's stability. Therefore, the velocity vector observed from plane 6 are quite symmetric without troublous flow. This state is different from flow separation phenomenon mentioned in Cheah's study due to the lack of swirl breaker.

A comparison of flow structure at impeller between design and off-design operating condition is demonstrated in Figure 6. As the flow enters the impeller eye, it is divided into the blade-to-blade passage. By dint of unsteady effect formed upstream, the flow coming into passages is no longer tangential to the leading edge of the blade. It can be found that at the flow rate $0.5Q_{design,}$ there is a large flow recirculation in two passages near tongue area.

Because of the volute tongue geometry, the flow exiting the impeller outlet is blocked. Therefore, flow in this area can not behave as usual like that in other passages. Moreover, in this case a flow separation at leading edge is also observed. Separation phenomenon results in an appearance of low velocity regions on the suction side of impeller blade which is well known as stall flow. It is considered as jet-wake structure and is reported in a number of studies. This flow condition can contribute to the

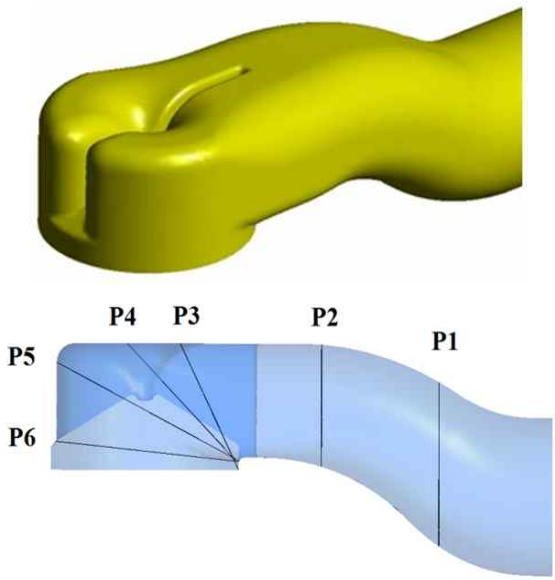

Fig. 4. Geometry of pump's suction.

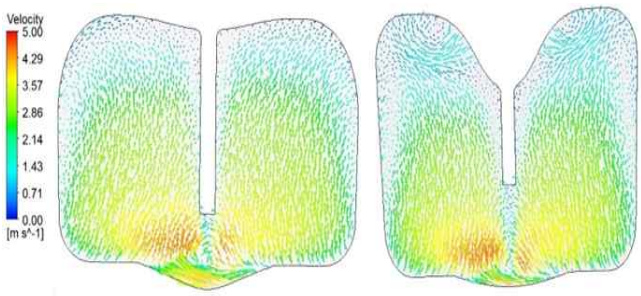

Plane 3 Plane 4

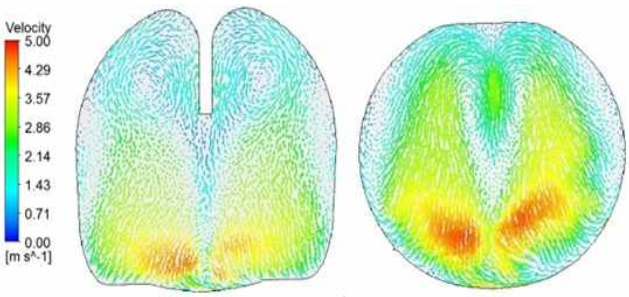

Plane 5 Plane 6

Fig. 5. Vortex formation at some positions in suction domain.

cavitation at blade suction side which is popular discussed in literature. The leading edge separation also takes responsibility of energy loss in the pump and affects the flow field within impeller passage in streamwise direction.

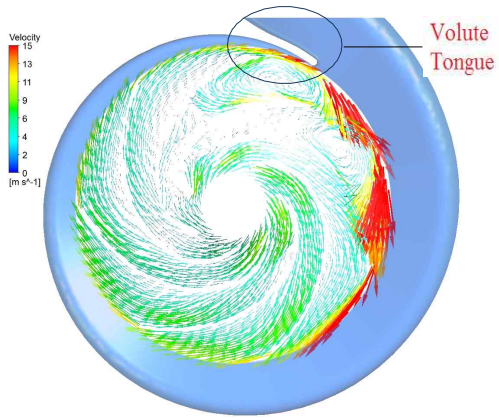

(a) 0.5 Qdesign

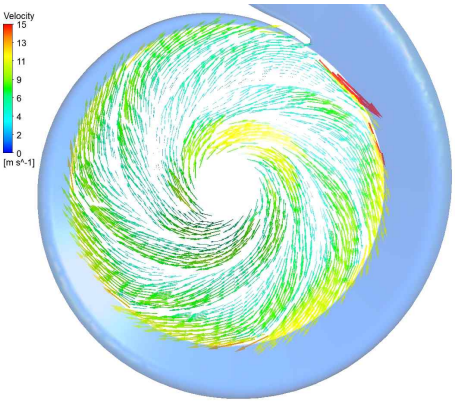

(b) Qdesign

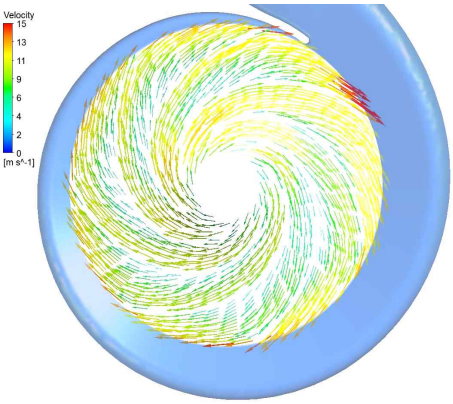

(c) 1.4 Qdesign

Fig. 6. Velocity vector at mid span of impeller at different flow rate.

On the other hand, the impeller passage flow at Q_{design} and $Q/Q_{design} = 1.4$ is generally smooth and no circulation flow is detected at any passage of impeller. At design flow rate there is a slightly higher velocity at trailing edge of near tongue passage. Meanwhile, in case of high flow rate velocity distribution in all

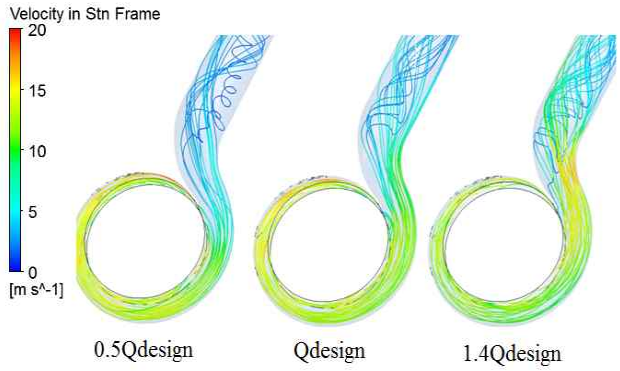

Fig. 7. Spiral vortex flow inside the volute.

passages is almost same as the others. In both circumstances, the flow follows the blade curvature profile from impeller passage entrance to the exit without any separation on suction or pressure side. That matches the potential flow theory for flow passing turbo machinery blade.

Figure 7 shows the difference in streamline or flow pattern at volute area in three working conditions. The most significant feature can be seen is that for all cases the flow within the volute before throat is quite smooth and uniform. The remarkable discrepancy is observed in the region from tongue to volute nozzle. There, the streamline at design flow rate is smooth, attacks to curvature of volute outer wall. As compared to off-design operations ($0.5Q_{design}$ and $1.4Q_{design}$), streamline is much more complex and troublous. The former, which lacks of momentum, witnesses a strong recirculation flow at volute nozzle. Whereas, the latter experiences a considerable backflow behind volute tongue, at this zone the flow is blocked and stalled. It is clear that the flow behind the volute tongue splits into two parts: stratified flow attached volute outer wall and spiral vortex flow near inner wall.

4.3 Pressure distribution

The pressure distribution on mean plane (at middle of impeller, normal to rotating axis) within impeller and volute domain is shown on Figure 8.

The first highlight on this figure is a drop of outlet pressure at volute throat as the flow rate increases. In other word, the higher flow rate is, the lower outlet pump head is. At lower and BEP, more positive pressure is observed near the volute outlet than around volute casing. In case of lower flow rate, there is an excessive pressure gradient at trailing edge region of blade near volute tongue. Turning to higher flow rate, pressure disposition for whole volute casing nearly does not change.

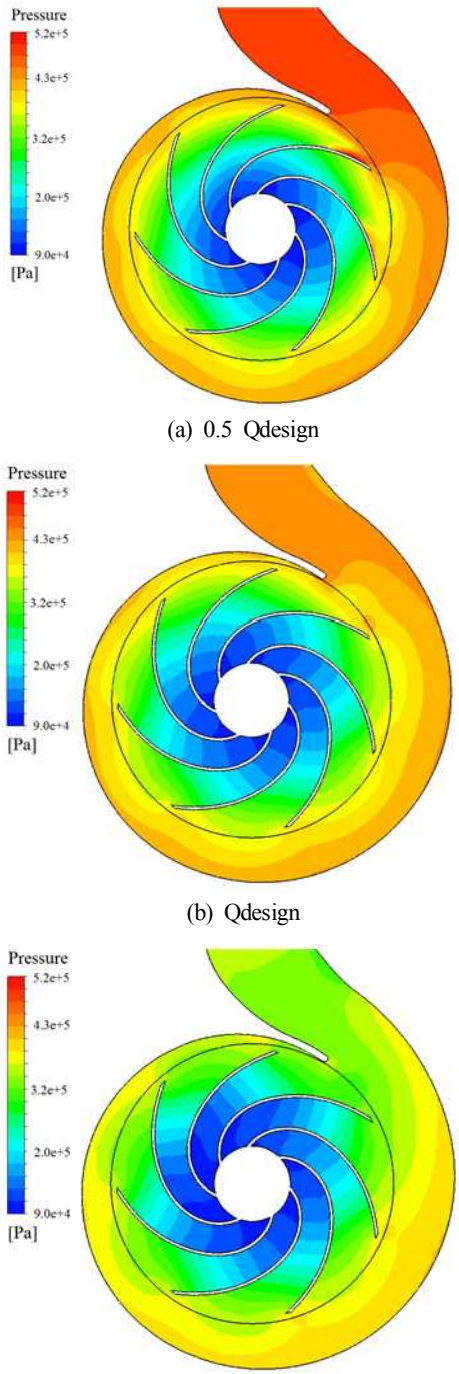

(a) 0.5 Qdesign

(b) Qdesign

(c) 1.4 Qdesign

Fig. 8. Pressure distribution at different flow rate.

For both design and off-design flow rate, a relatively uniform pressure distribution is obtained around the impeller despite the impact of volute tongue. The pressure rises gradually along streamwise direction within impeller blade-to-blade passage. At the same distance from impeller center, pressure side possesses a higher pressure than suction surface for all passages. After discharging from impeller outlet, the flow enters, going along spiral volute which is equipped in order to convert a part of fluid dynamic energy to pressure energy. For this reason, it reaches the highest pressure after passing volute throat, remaining pressure value until pump outlet.

5. Conclusion

CFD code has proved its outstanding advantage in simulation and visualization complicated internal flow inside a centrifugal pump. The complex flow is analyzed in a wide range of flow rate by employing numerical computation. The predicted pump head and efficiency are in good arrangement with experimental ones. Two simulating performance curves follow same trend as actual characteristic curves with quite small disparity. Therefore, CFD simulation offers a great opportunity to obtain a comprehensive understanding of complex internal flow pattern as well as velocity and pressure distribution of the pump at design and off-design condition.

The formation of swirl flow is unavoidable within suction domain. Nonetheless, swirl breaker is able to play an essential role in diminishing harmful effects of vortex on flow's stability before entering impeller eye.

At BEP, the velocity vector and streamline are very smooth along the curvature of impeller blade. Meanwhile, the flow features considerably change when the pump operates at off-design condition. The flow pattern is no longer well-behaved as at design point. At lower flow rate, a strong flow recirculation exists within the impeller passage near tongue area. This causes stall phenomenon which blocks the flow through the passage.

In terms of pressure distribution, the pressure progressively increases follow direction of streamwise. In general, volute outlet pressure falls according to the raise of pump flow rate. A relatively uniform of pressure distribution is also found on mid-plane when the pump works at design flow rate.

Nomenclature

d_1	Impeller inlet diameter [m]
d_2	Impeller outlet diameter [m]
g	Gravity acceleration [m/s^2]
H	Pump Head [m]
N	Rotational speed [rad/s]

Q	Flow rate [m^3/h]
Q_{design}	Design flow rate [m^3/h]
Ψ	Non-dimensional head coefficient (= $gH/N^2d_2^2$)
ϕ	Non-dimensional flow coefficient (= Q/Nd_2^3)
N_s	Specific speed (= $N\sqrt{Q}/(gH)^{3/4}$)
BEP	Best efficiency point
NPSH	Net positive suction head [m]

References

[1] Asuaje, M., F. Bakir, G. Kergourlay, R. Noguera and R. Key (2006), Three-dimensional Quasi-steady flow simulation in a centrifugal pump: Comparision with experiment results, Journal of Power and Energy, Vol. 220, pp. 239-256.

[2] Bacharoudis, E. C., A. E. Filios, M. D. Mentzos and D. P. Margaris(2008), Parametric study on a centrifugal pump impeller by varying the outlet blade angle, The Open Mechanical Engineering Journal, No. 2, pp. 75-83.

[3] Byskov, D. R. K., C. B. Jacobsen and N. Pedersen(2003), Flow in a centrifugal pump impeller at design and off-design condition-part II: large eddy simulations, ASME Journal of Fluid Engineering, Vol. 125, No. 1, pp. 73-83.

[4] Cheah, K. W., T. S. Lee and S. H. Winoto(2011), Numerical study of Inlet and Impeller flow structure in a centrifugal pump at design and off-design points, International Journal of Fluid machinery and System, Vol. 4, No. 1, pp. 182-191.

[5] Ferziger, J. H. and M. Peric(1996), Computational Method of Fluid Dynamics, Springer, Berlin, Germany.

[6] Gu, F., A. Engeda, M. Cave and J. L. Diliberti(2001), A numerical investigation on the volute/diffuser interaction due to axial distortion at the impeller exit, ASME Journal of Fluid Engineering, Vol. 123, No. 3, pp. 475-483.

[7] Majidi, K. and H. E. Siekmann(2000), Numerical simulation of secondary flow in pump volute and circular casing using 3D viscous flow techniques, International Journal of Rotating Machinery, Vol. 6, No. 4, pp. 245-252.

Received : 2016. 12. 29.
Revised : 2017. 02. 22.
Accepted : 2017. 02. 25.